

University of Montana

ScholarWorks at University of Montana

Graduate Student Theses, Dissertations, &
Professional Papers

Graduate School

1969

Kinetics and mechanism of the thermal decomposition of sodium monohydrogen phosphate

Anthony Cheong-Ngai Chang
The University of Montana

Follow this and additional works at: <https://scholarworks.umt.edu/etd>

Let us know how access to this document benefits you.

Recommended Citation

Chang, Anthony Cheong-Ngai, "Kinetics and mechanism of the thermal decomposition of sodium monohydrogen phosphate" (1969). *Graduate Student Theses, Dissertations, & Professional Papers*. 7586. <https://scholarworks.umt.edu/etd/7586>

This Thesis is brought to you for free and open access by the Graduate School at ScholarWorks at University of Montana. It has been accepted for inclusion in Graduate Student Theses, Dissertations, & Professional Papers by an authorized administrator of ScholarWorks at University of Montana. For more information, please contact scholarworks@mso.umt.edu.

KINETICS AND MECHANISM OF THE THERMAL DECOMPOSITION
OF SODIUM MONOHYDROGEN PHOSPHATE

By

Anthony Cheong-Ngai Chang

B.Sc. Taiwan Provincial Cheng Kung University, 1961

Presented in partial fulfillment of the requirements
for the degree of

Master of Science

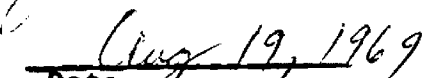
UNIVERSITY OF MONTANA

1969

Approved by:


Chairman, Board of Examiners


Dean, Graduate School


Date

UMI Number: EP38387

All rights reserved

INFORMATION TO ALL USERS

The quality of this reproduction is dependent upon the quality of the copy submitted.

In the unlikely event that the author did not send a complete manuscript and there are missing pages, these will be noted. Also, if material had to be removed, a note will indicate the deletion.



UMI EP38387

Published by ProQuest LLC (2013). Copyright in the Dissertation held by the Author.

Microform Edition © ProQuest LLC.

All rights reserved. This work is protected against unauthorized copying under Title 17, United States Code



ProQuest LLC.
789 East Eisenhower Parkway
P.O. Box 1346
Ann Arbor, MI 48106 - 1346

ACKNOWLEDGMENTS

It is a pleasure to express my gratitude to Professor R. Keith Osterheld for his guidance and patience throughout this research and in the preparation of the manuscript.

Thanks are also given to Mr. Ronald Susott for his many helpful discussions.

TABLE OF CONTENTS

	Page
ACKNOWLEDGMENTS - - - - -	i
LIST OF TABLES- - - - -	iii
LIST OF FIGURES - - - - -	iv
CHAPTER	
I. Introduction - - - - -	1
II. General Aspects of Solid Decomposition - - - - -	3
III. Theory	
A. Nucleation - - - - -	6
B. Propagation- - - - -	8
C. Complete Rate Expressions- - - - -	8
IV. Experimental Methods	
A. Instrumentation- - - - -	15
B. Preparation of Samples - - - - -	18
C. Procedure- - - - -	20
V. Results	
A. Effects of Particle Size - - - - -	23
B. Separation of the Reaction Stages- - - - -	27
C. Kinetic Studies of Samples of 40-65 Mesh - - - - -	29
D. Kinetic Studies for Samples of Very Fine Powder - - - - -	35
VI. Discussion	
A. The Erofeev Mechanism- - - - -	42
B. The Logarithmic Decay Mechanism- - - - -	44
C. Interpretation of Activation Energies- - - - -	49
SUMMARY - - - - -	53
BIBLIOGRAPHY- - - - -	54

LIST OF TABLES

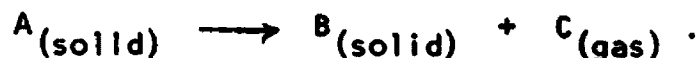
TABLE	Page
I. Fractional Decomposition (α) Value at the Rate Minimum for Different Particle Sizes- - - -	26
II. Fractional Decomposition (α) Value at the Rate Minimum as a Function of Temperature for Na_2HPO_4 (270-325 mesh) - - - - -	26
III. Data and Values of Different Kinetic Functions Tested for Reaction of Na_2HPO_4 (40-65 mesh) at 608°K- - - - -	30
IV. Prout-Tompkins Kinetic Constant at Various Temperatures for Na_2HPO_4 (40-65 mesh)- - - - -	32
V. Erofeev Kinetic Constant at Various Temperatures for Na_2HPO_4 (40-65 mesh)- - - - -	33
VI. Data and Values of Different Kinetic Functions Tested for Reaction of Na_2HPO_4 (very fine powder) at 588°K - - - - -	36
VII. Decay Kinetic Constant at Various Temperatures for Na_2HPO_4 (very fine powder)- - -	38
VIII. Activation Energies in the Na_2HPO_4 Decomposition- - - - -	51

LIST OF FIGURES

FIGURE	Page
1. Typical Thermal Decomposition Curves - - - - -	4
2. Diagram of Spherical Interfacial Reaction- - - -	12
3. Diagram of Diffusion Controlled Reaction - - - -	13
4. Block Diagram of DSC-1B - - - - -	16
5. Diagram of the New Cell Cover- - - - -	19
6. Thermal Scans of Na_2HPO_4 - - - - -	24
7. Thermograms of Na_2HPO_4 at 604°K - - - - -	25
8. Thermogram of Na_2HPO_4 (40-65 mesh) - - - - -	28
9. Kinetic Expression of Na_2HPO_4 (40-65 mesh) at 608°K - - - - -	31
10. Arrhenius Plot for Na_2HPO_4 (40-65 mesh)- - - - -	34
11. Thermograms of Na_2HPO_4 (very fine powder) at 588°K - - - - -	37
12. Kinetic Plot of Na_2HPO_4 (very fine powder) at 588°K - - - - -	39
13. Arrhenius Plot for Na_2HPO_4 (very fine powder)- -	40
14. Thermogram obtained from a Combination of the Decay and Erofeev Kinetics - - - - -	47

I. INTRODUCTION

An important class of thermal decompositions of solids consists of those reactions of the form:



The kinetic data concerning a solid decomposition are generally expressed in the form of (a) the fractional decomposition (α) as a function of time (t) or temperature (if the reaction is performed under an uniform heating rate), or (b) the rate of fractional decomposition ($\frac{d\alpha}{dt}$) as a function of time or temperature.

Several commercial instruments are available for obtaining these data. Commonly used are:

(a) Differential Thermal Analysis (DTA)--In this technique one measures the differential temperature between the sample and an inert reference material in a furnace heated at a constant rate.

(b) Thermogravimetric Analysis (TGA)--For this one measures the weight loss of the reactant as a function of time or temperature.

(c) Differential Scanning Calorimetry (DSC)--This technique measures the differential energy required to maintain the same temperature in the sample and reference as the two are maintained isothermally or are heated at a uniform rate.

(d) Gas Evolution Detection (GED)--One measures the rate of the evolution of the gaseous decomposition products as a function of time, generally by measuring the thermal conductivity of the carrier gas leaving the cell in which the decomposition is occurring.

(e) Pressure Change Method--One measures the pressure of the gaseous decomposition product(s) as a function of time in a constant volume system.

The effect of temperature on reaction rate may be seen from the Arrhenius equation:

$$k = Ae^{-\Delta E^*/RT} \quad (1)$$

where k is the reaction rate at constant temperature T , A is the frequency factor (generally independent of temperature), ΔE^* is the Arrhenius activation energy and R the gas constant. In the study of a particular thermal decomposition, the reaction rate constants (k) at different temperatures are calculated from experimental data; the activation energy can then be obtained from equation 1. The rate constant k can be obtained from data of either a thermal scan or an isothermal run. Since data from a thermal scan include one more temperature parameter, the mathematics involved in the kinetic expressions (see Theory below) are more complicated. In the present study we will concentrate on isothermal reactions.

II. GENERAL ASPECTS OF SOLID DECOMPOSITION

In general the decomposition curves (α vs. t) obtained in an isothermal run can be classified in four types as shown in Figure 1.⁵ Type (a) is a sigmoid curve, indicating an autocatalytic reaction. In (b) the acceleratory period is relatively short, most material reacts in the decay period. In (c) no induction period occurs. Curve (d) shows, in addition to a sigmoid, a small evolution of gas at the beginning of the reaction. In general, grinding a crystal or scratching the surface of a crystal will reduce the induction period. The corresponding graphs of $d\alpha/dt$ vs. t also appear in Figure 1.

Any of these types of decomposition curves can be explained in terms of nucleation and propagation. At the start of a reaction, due to lattice imperfection (lattice defects, dislocations, etc.) on the surface of the crystals, a number of active nuclei are formed at those places where the activation energy is least. A growth nucleus, depending upon the nature of the experimental material, may take several intermediate steps to form. After the formation of a growth nucleus, it starts to grow. This process of nuclei growth is called propagation.

In the kinetic study of a particular solid decomposition, kinetic equations in terms of α (or $\frac{d\alpha}{dt}$) and t are derived based on certain assumptions concerning nucleus formation and growth.

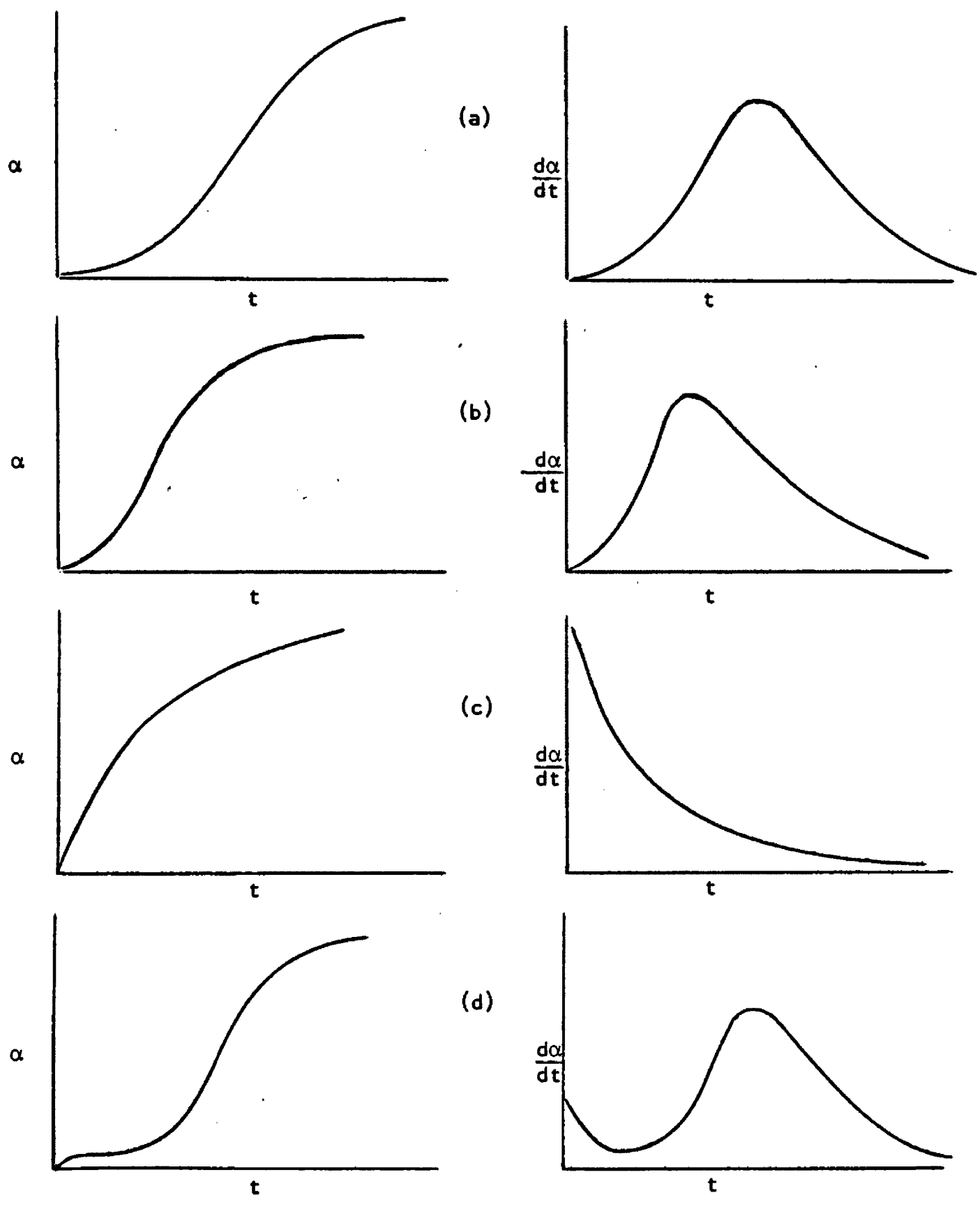


Figure 1--Typical thermal decomposition curves

Should only one of these formulas fit the experimental data, we conclude that the reaction follows the assumptions that lead to that kinetic equation.

III. THEORY

Many equations for different kinetic assumptions appear in the literature; only those that had to be considered in the present investigation will be considered here. For other theories the interested reader can refer to references 5 and 15, and current literature.

A. Nucleation

Suppose the reactant contains N_0 nucleus forming sites which are of slightly lower chemical stability than the remainder of the crystal. The rate of nucleation is then proportional to the number of points which remain inactivated at time t . The rate of nucleation is

$$\frac{dN}{dt} = k(N_0 - N) \quad (2)$$

where N is the number of nuclei at time t , and k the proportionality constant. From equation 2 we have

$$\int_0^N \frac{dN}{N_0 - N} = k \int_0^t dt$$

and

$$N = N_0(1 - e^{-kt}) \quad (3)$$

Substitute equation 3 into equation 2 and we get

$$\frac{dN}{dt} = kN_0 e^{-kt} \quad (4)$$

This is called the Exponential Law of Nucleation. If k is small, we may expand the exponential term and neglect higher powers than kt to obtain:

$$N = kN_0t$$

and

$$\frac{dN}{dt} = kN_0 \quad (5)$$

This case, in which the number of nuclei increases linearly with time, is called the Linear Law. If k is very large, instantaneous nucleation occurs, i.e.

$$N = N_0$$

All the nucleation laws mentioned above involve only one step. Nucleation processes involving more than one step are also known. Bagdasar'yan² has shown that if β successive steps with probabilities k_1, k_2, \dots, k_β are required to form an active growth nucleus, the number of nuclei at time t is

$$N = \frac{k_1 k_2 \dots k_\beta N_0}{\beta!} t^\beta = Dt^\beta \quad (6)$$

For example, if a combination of two intermediaries is involved in forming a growth nucleus, and the number of each active intermediate at time t is $k't$ (i.e. using the Linear Law of Nucleation to describe the rate of appearance of the intermediates), provided there is no reverse reaction and k , their rate of combination to

form nuclei, is small compared with k' , the rate of nucleus formation is then

$$\frac{dN}{dt} = k(k't)^2$$

so that

$$N = \frac{kk'^2}{3} t^3 \quad (7)$$

In this example, three steps are required and β has the value three; two steps are the appearance of the two intermediates required and the third step is their combination. Consequently if β steps are required to form a growth nucleus then the Power Law (eq. 6) is obtained.

B. Propagation

After a growth nucleus is formed, it starts to grow in one, two or three dimensions. In general, we can express the growth of a nucleus as a function of volume (v) and time (t):

$$v = \sigma(k_g t)^\lambda \quad (8)$$

where σ is a shape factor, equal to $\frac{4\pi}{3}$ for a spherical nucleus; k_g is the propagation rate constant and λ is equal to 1, 2 or 3 for one-, two- or three-dimensional growth, respectively.

C. Complete Rate Expressions

1. The Power Law. In this kind of thermal decomposition kinetics the nucleation process according to equation 6 is assumed:

$$\frac{dN}{dt} = D\beta t^{\beta-1} \quad (6)$$

If the growth of a nucleus starts at time $t=y$ and the overlap between growing nuclei is not considered, then the total size of all nuclei at time t is

$$V(t) = \int_0^t \sigma [k_g(t-y)]^\lambda \left[\frac{dN}{dt} \right]_{t=y} dy \quad (9)$$

Substituting $\frac{dN}{dt}$ from equation 6 and changing t to y , we obtain

$$V(t) = \int_0^t \sigma [k_g(t-y)]^\lambda D \beta y^{\beta-1} dy$$

or

$$V(t) = \sigma k_g^\lambda D t^{\beta+\lambda} \left[1 - \frac{\lambda \beta}{\beta+1} + \frac{\lambda(\lambda-1)}{2!} \frac{\beta}{\beta+2} \dots \right]$$

$$\lambda \leq 3 \quad (10)$$

Since $V(t)$ is proportional to α , finally we have

$$\alpha = C t^{\beta+\lambda} \quad (11)$$

The fractional decomposition is proportional to a power of time, equation 11 is called the Power Law.

2. Erofeev Equation. In equation 11 we have not considered overlap and ingestion between growing nuclei. As the nuclei grow larger they must impinge upon each other and the growth will stop at the point at which they touch. The factor $(1-\alpha)$ is commonly used to correct the rate for this effect.¹ From equation 11 we get

$$\frac{d\alpha}{dt} = (\beta+\lambda) C t^{(\beta+\lambda)-1} \quad (12)$$

Entering the $(1-\alpha)$ correction factor in the usual way we obtain

$$\frac{d\alpha}{dt} = (\beta+\lambda)Ct^{(\beta+\lambda)-1}(1-\alpha) \quad (13)$$

Integration of (13) gives the Erofeev Equation⁴

$$\begin{aligned} \alpha &= 1 - \exp - [Ct^{(\beta+\lambda)}] \\ &= 1 - \exp - (kt)^n \end{aligned} \quad (14)$$

where $n = \beta + \lambda$ and $k = C/(\beta + \lambda)$. For a reaction that shows Erofeev kinetics a plot of $[\log(\frac{1}{1-\alpha})]^{\frac{1}{n}}$ vs. t will give a straight line with slope equal to k . The value of n is the sum of the number of steps in formation of a growth nucleus and the number of dimensions of propagation.

3. Prout-Tompkins Equation. The development of the Prout-Tompkins equation is based on the concept of nuclei as linear, branching chains introduced by Garner and Hailes.⁶ In addition to a constant rate of nucleation (k_1) at N_0 potential sites, a large number of nuclei are formed by the chain mechanism. In effect many points on the propagation chain are effective nuclei at which branching can occur; if the probability of branching is k_2 , the rate of nucleation at time t is then

$$\frac{dN}{dt} = k_1N_0 + k_2N \quad (15)$$

In Garner's equation (eq. 15) the interference between the branching chains is neglected. This may be corrected by including

a new term in equation 15 for the probability of chain termination (k_3). Thus

$$\frac{dN}{dt} = k_1 N_0 + k_2 N - k_3 N \quad (16)$$

If k_1 is very large, the N_0 potential sites are soon exhausted and we may neglect the first term in equation 16. We may then write

$$\frac{dN}{dt} = (k_2 - k_3)N = k'N \quad (17)$$

Alternatively if k_1 is small the branching process still predominates and $(k_2 - k_3)N \gg k_1 N_0$, equation 17 is still valid. At any instant the rate of decomposition ($\frac{d\alpha}{dt}$) may be assumed to be proportional to the number of nuclei present, i.e.

$$\frac{d\alpha}{dt} = (k_2 - k_3)N = k'N \quad (18)$$

Equations 17 and 18 cannot be integrated unless we know the probabilities k_2 and k_3 as a function of α . Prout and Tompkins¹² consider the case of a symmetrical sigmoid for which the point of inflection is at $\alpha_i = \frac{1}{2}$. At $t = 0$, $\alpha = 0$ and k_3 must be zero, because interference at zero time is not possible. While at $t = t_i$, $\alpha = \alpha_i$, $\frac{d\alpha}{dt} = 0$ and $k_2 = k_3$. These boundary conditions can be satisfied by the assumption

$$k_3 = k_2 \frac{\alpha}{\alpha_i} \quad (19)$$

Thus from equation 17

$$\frac{dN}{dt} = k_2 \left(1 - \frac{\alpha}{\alpha_i}\right) N \quad (20)$$

Using equation 18 we have

$$\frac{dN}{dt} = \frac{k_2}{k_1} \left(1 - \frac{\alpha}{\alpha_i}\right) \frac{d\alpha}{dt}$$

or

$$\frac{dN}{d\alpha} = \frac{k_2}{k_1} \left(1 - \frac{\alpha}{\alpha_i}\right) \quad (21)$$

Integration of equation 21 gives

$$N = \frac{k_2}{k_1} \left(\alpha - \frac{\alpha^2}{2\alpha_i}\right) \quad (22)$$

Substituting equation 22 into equation 18 and setting $\alpha_i = \frac{1}{2}$ we obtain

$$\frac{d\alpha}{dt} = k_2 \alpha (1-\alpha) \quad (23)$$

Further integration gives the Prout-Tompkins equation

$$\log\left(\frac{\alpha}{1-\alpha}\right) = k_2 t + \text{constant} \quad (24)$$

4. Spherical Interfacial Equation.¹³ Suppose the geometrical form of a crystal is a sphere of radius R , and nucleation occurs instantaneously and uniformly over the entire surface of the crystal. The fraction of material remaining unreacted at time t is then

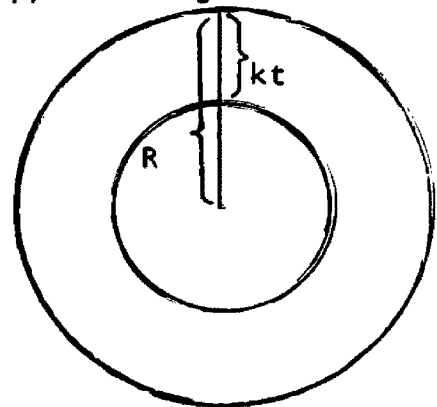


Figure 2

$$1 - \alpha = \frac{\frac{4}{3}\pi(R-kt)^3}{\frac{4}{3}\pi R^3} \quad (25)$$

where k is the linear proportional constant, the rate of advance of the reactant/product interface. Rearrangement of equation 25 gives

$$(1 - \alpha)^{\frac{1}{3}} = 1 - \frac{k}{R}t \quad (26)$$

It can be shown that this expression is valid for particles of any chunky shape, not necessarily spherical.

5. Diffusion controlled Equation. Based on the assumption that the rate of diffusion of the gaseous product(s) through the reacted material is inversely proportional to the thickness of the reacted material, Jander⁹ derived an expression for the rate of reaction for a spherical particle

$$[1 - (1-\alpha)^{\frac{1}{3}}]^2 = \frac{k}{R^2}t \quad (27)$$

The above equation can easily be obtained by setting

$$\frac{dl}{dt} = \frac{k'}{l} \quad (28)$$

where k' is the diffusion constant, and l the thickness of the reacted material. Integration of the equation 28 gives

$$l = (2k't)^{\frac{1}{2}} = (kt)^{\frac{1}{2}}$$

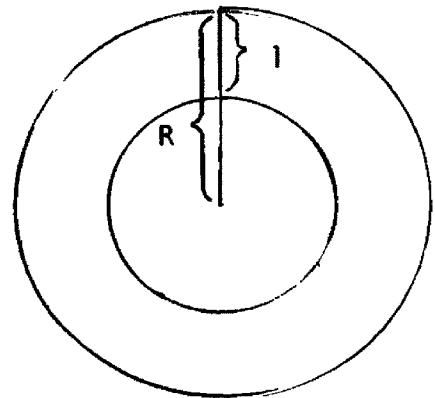


Figure 3

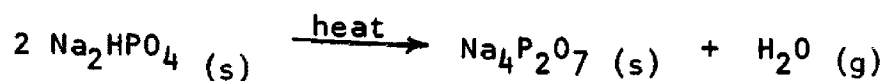
Paralleling equation 25 we have

$$1 - \alpha = \frac{[R - (kt)^{\frac{1}{2}}]^3}{R^3} \quad (29)$$

This gives formula 27 immediately.

IV. EXPERIMENTAL

In the present investigation, the decomposition of Na_2HPO_4 was studied at 300-345°C.



Samples were heated isothermally in a Differential Scanning Calorimeter (DSC) at the desired temperature at atmospheric pressure in a stream of inert gas (N_2). By means of a thermal conductivity cell in the effluent gas stream the partial pressure of water and, hence, the rate of the evolution of the constitutional water was measured. The instrument used and the procedure employed will be considered in more detail below.

A. Instrumentation

The Differential Scanning Calorimeter-1B (Perkin-Elmer Co.) consists of two holders, one for the reactant, another for an inert reference material. A platinum resistance thermometer and a heater are installed in the base of each holder. The machine is designed to measure the differential energy required to maintain both holders at the same temperature while both holders are heated at a constant rate or are held at the same constant temperature. The operating principle^{8,14} of the DSC is divided into two loops as shown in Figure 4.

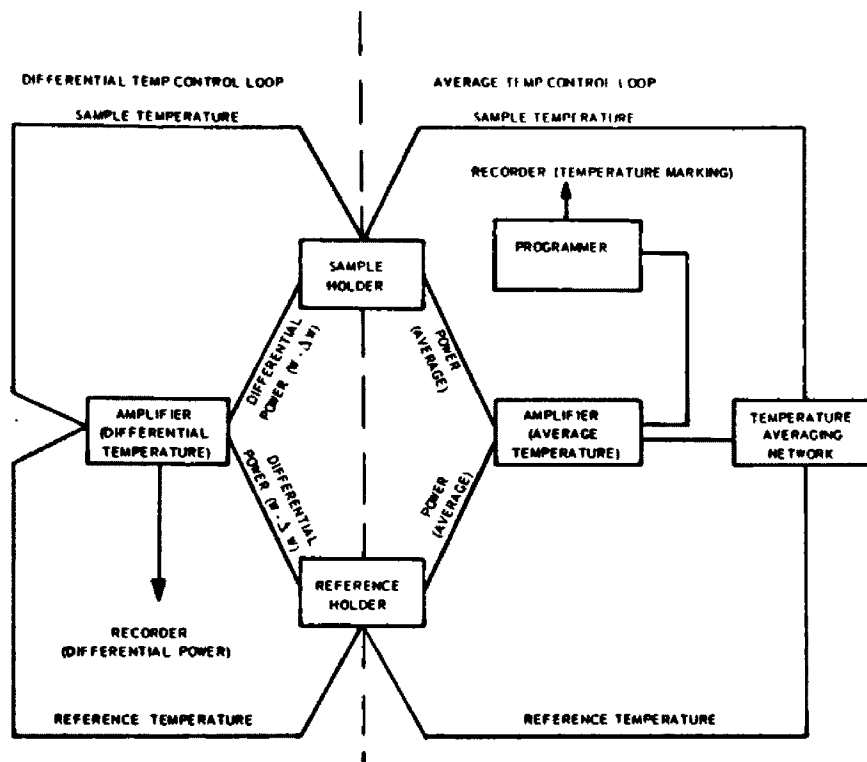


Figure 4--Block Diagram of DSC-1B (Perkin-Elmer Co.)

In the temperature control loop the programmer feeds in a signal, which is proportional to the temperature of both sample and reference holders, to the amplifier. The signal when it reaches the amplifier, is compared with another signal from the thermometers of the holders via an average temperature computer. If the temperature demanded by the programmer is higher than the average temperature of the sample and reference holders, more heating current will be supplied to the heaters. If the average temperature of the holders is higher, current to the heaters will be decreased. In this way the temperature of the two holders is rapidly adjusted to the temperature called for by the programmer.

In the like manner, the differential temperature control loop compares the signals representing the sample and reference temperatures. Depending upon whether the sample or the reference temperatures is greater, an adjusted difference in power is fed to the heaters to eliminate the temperature difference between them. A signal proportional to this differential power is transmitted to a recorder. However, due in part to the mass and heat capacity differences between the sample and reference containers, this signal is so large that it is not useful at the start of an isothermal run for which the pre-heat temperature is safely below the reaction temperature.

Because the DSC data were not useful in the beginning of an isothermal run, in our studies the DSC machine was used only for temperature control. The manufacturer claims a temperature reproducibility of $\pm 0.1^{\circ}\text{C}$. Reaction rates were measured by an Effluent Gas Analyzer (see next paragraph). Lead metal (m.p. 600°K) was used to calibrate the temperature dial to read $600.0^{\circ}\text{K} \pm 0.1^{\circ}\text{K}$ at the lead melting point. Over the relatively narrow temperature range used around 600°K the temperature uncertainty can be considered to be $\pm 0.1^{\circ}\text{C}$.

The DSC includes an Effluent Gas Analyzer (EGA) unit. In this unit a two-thermistor bridge (detector) is used to detect carbon dioxide, water vapor and other gaseous decomposition products by their influence on the thermal conductivity of the sweeping gas stream leaving the cell. A gas stream such as nitrogen or helium

is used to sweep out the cell cavity and to carry all gaseous products to the detector. From the detector a signal representing the composition of the effluent gas is transmitted to a recorder.

In our studies, the only volatile decomposition product was water. The detector signal was proportional to the water vapor concentration in the nitrogen carrier stream. At a constant carrier flow-rate, this concentration was directly proportional to the reaction rate. The detector signal, then, was directly proportional to the reaction rate. It was found that under normal operation, using the carrier gas flow rate of ≈ 30 ml/min recommended by the manufacturer and the cell cover provided, the EGA signal did not match the DSC signal exactly. This seemed to be due to the diffusion of water vapor into the hollow space of the metal cell cover (27 ml). Fast changes in the rate of evolution of the water vapor were thus averaged somewhat before they reached the detector. In order to reduce the empty space a new cell cover was built. This new cover (Fig. 5) had a volume of 15 ml. With this reduced volume and an increase in the carrier gas flow rate to 70 ml per minute, the carrier gas could sweep out the gaseous product fast enough to give EGA curves which matched the DSC curves (except for the early part of the DSC curve where the DSC signal was not useful, of course).

B. Preparation of Samples

The sodium monohydrogen phosphate used was from Mallinckrodt Chemical Company, Lot No. 7917. Samples of moderate size particles

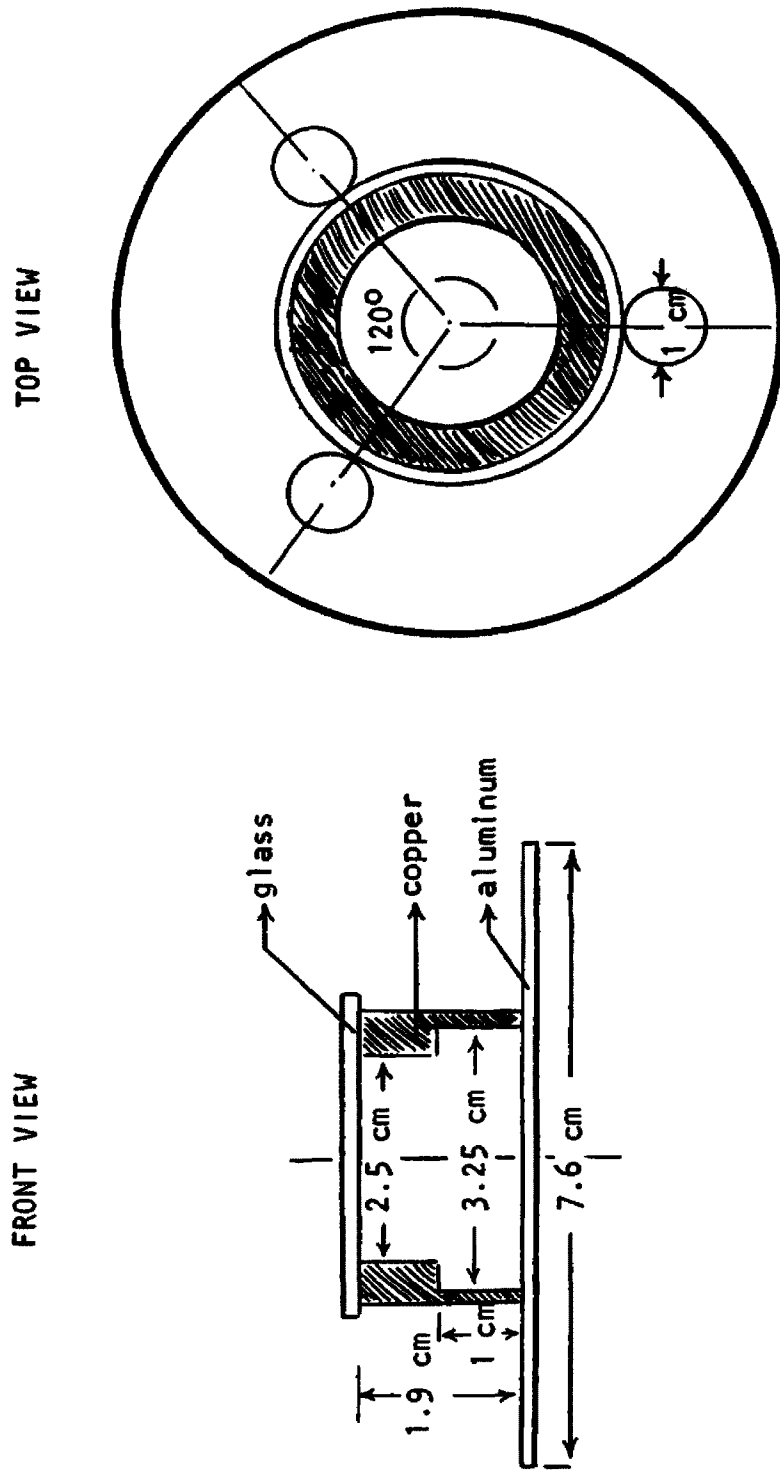


Figure 5--Diagram of the new cell cover.

and of very fine powder were prepared as follows:

1. The commercial product was ground to moderate size particles. By means of sieves the sample was separated into 40-65, 100-115, 115-150, 150-170, 170-200, 200-270 and 270-325 mesh particle size ranges. For each sample acetone was used to wash out all powder attached to the surface of the particles. The samples were heated at 110-125°C in an oven for two hours. Under the microscope the particles of each sample looked transparent and chunky in shape.

2. To obtain a sample of very fine powder, 40-65 mesh Na_2HPO_4 and a metal bead were put into a small plastic bottle. A Wig-L-Bug (Crescent Dental Mfg. Co.) was used to shake the bottle for five minutes. Powdered Na_2HPO_4 in the plastic bottle was put into 40 ml of methanol and stirred vigorously for half a minute. The mixture was allowed to settle for one minute and then the supernatant liquid was decanted. The decanted mixture was allowed to stand for two minutes and then the supernatant liquid was decanted again. The sample consisted of the particles that settled out during the two-minute interval. These particles were washed with acetone and then dried in an oven at 110-125°C for more than two hours.

C. Procedure

Throughout this study the Differential Scanning Calorimeter was used for heating purposes and for temperature control, using nitrogen as carrier gas. The sample (10-30 mg) to be decomposed

was put into an aluminum pan. An empty pan was used as reference. In order to increase the thermal contact between the sample and holder and to match the thermal emissivity of the sample pan and reference, both the sample pan and the reference pan were capped with an inner cover and a dome cover. Experiments by a co-worker (Ronald Susott), based on the apparent melting point of lead, showed that the top of an uncovered sample would be as much as 3°C below the temperature at the bottom of the sample. Except as reported in the next paragraph, all samples were preheated at 460°K for 10 to 15 minutes. This preheat temperature was 70°C lower than the temperature at which reaction could first be detected, and was approximately 140°C lower than the desired reaction temperature. The sample was held at the pre-heat temperature until all air in the heating assembly had been swept out by the nitrogen carrier gas, as determined by achieving a straight base-line in the EGA signal. The DSC temperature control was then manually dialed from the pre-heat temperature to the desired reaction temperature as rapidly as possible (about 10 sec.). In addition to this 10 second period, approximately one minute was required for the machine to reach the desired temperature. This was determined by dialing from the pre-heat temperature (460°K) to the melting point of lead (600°K) and timing the interval until a lead sample melted.

Instead of preheating at 460°K some samples of 40-65 mesh were treated differently. Before the sample was put in the

heating assembly the DSC was manually set at 580°K. This temperature was 50°C higher than the temperature at which the reaction started. The sample was then put on the sample holder and allowed to react for 10 to 15 minutes. The reaction rate at this time was very slow and a straight line was shown on the record of the EGA output. The DSC temperature control was then dialed to the desired reaction temperature (604-620°K). Less than half a minute was required for the machine to reach the desired temperature. This second preheat procedure, used in runs that will be identified later, was designed to eliminate a minor first stage reaction and to obtain more useful data for the early period of the main reaction.

In all runs, a flow of 80 ml/min (40-65 mesh runs) or 69 ml/min (very fine powder runs) of nitrogen was used to sweep the reaction cell and carry water vapor from the thermal decomposition zone to the thermal conductivity cell of the EGA analyzer. All rate data reported in this study were determined from the EGA signal from isothermal runs. The time at which this signal first departed from the baseline was considered to be zero time (t_0) for a run. Fractional decomposition (α) data were obtained by integrating the $\frac{d\alpha}{dt}$ vs. t graph. The recorder used was equipped with a Disc Integrator for the very fine powder runs. The integration was accomplished for the 40-65 mesh runs by tracing the curve and cutting and weighing.

V. RESULTS

A. Effects of Particle Size

The thermal decomposition kinetics of Na_2HPO_4 are affected remarkably by the sample particle size. All samples start to react about 530°K , but the smaller the sample particle size the greater the initial rate of the reaction. In Figure 6 thermal scans (reaction rate vs. temperature) of three different particle sizes are compared. In (a), for 40-65 mesh particles, a very slow reaction begins at 550°K , the reaction continues slowly to 602°K , and most material reacts at 602 - 620°K . In (b), for 270-325 mesh particles, reaction starts at 530°K with the rate increasing up to 605°K . From this point the reaction rapidly becomes faster and reaches a maximum rate at 619°K , following which the rate decreases rapidly. In (c), for very fine powder, the reaction begins at 520°K . The reaction rate keeps increasing markedly to a maximum at 623°K , and then decreases rapidly.

For isothermal runs more or less the same result is obtained. Figure 7 shows thermograms of samples of different particle size reacting isothermally at 604°K . The first hump in the thermogram becomes larger as a sample of smaller particle size is used; finally a one-hump curve is obtained for the sample of very fine powder. The time that the reaction takes to reach the second maximum rate is not strongly dependent on particle size. The fractional

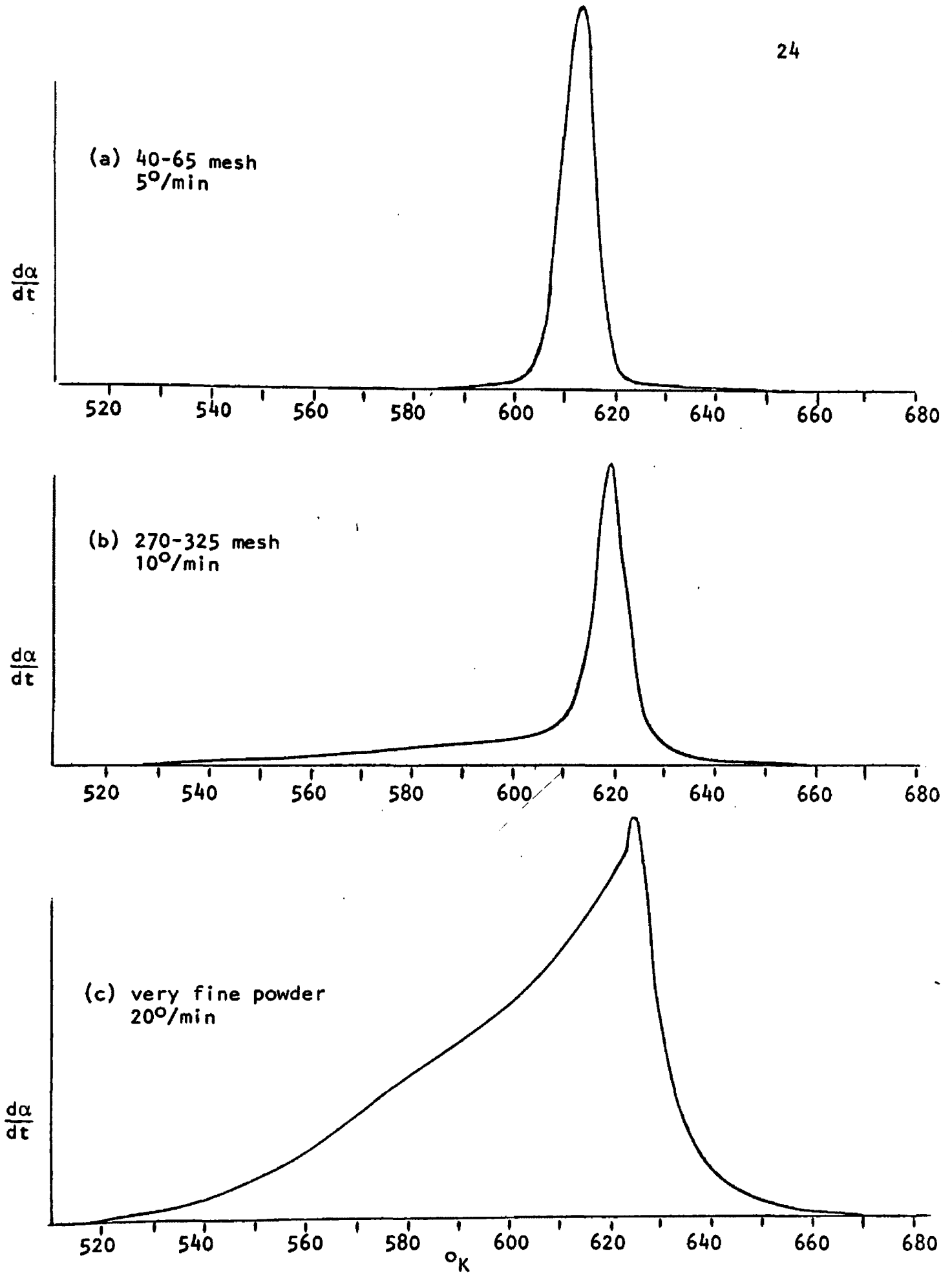


Figure 6--Thermal scans of Na_2HPO_4 $\frac{d\alpha}{dt}$ vs. T

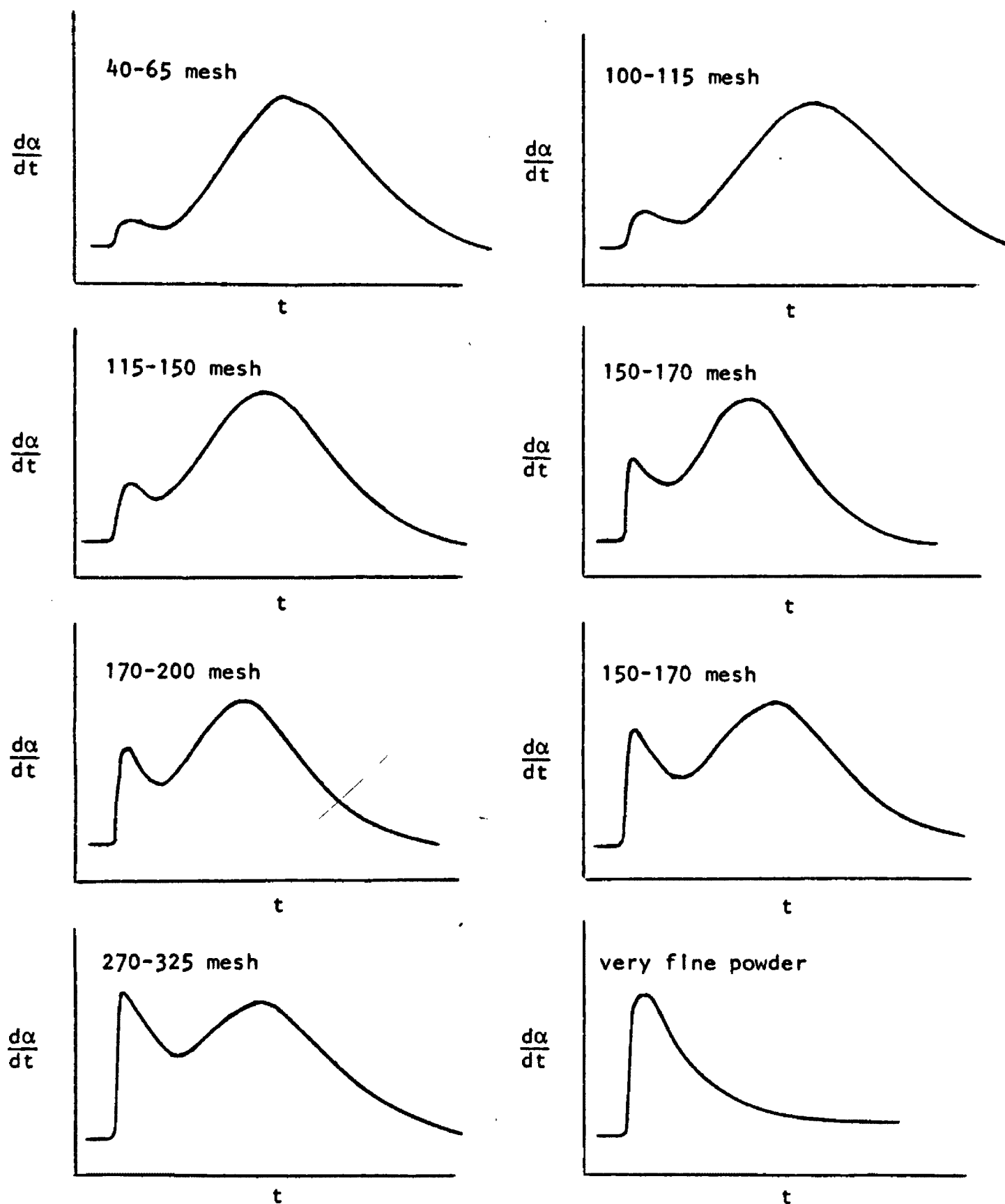


Figure 7--Thermograms of Na_2HPO_4 at 604°K

decomposition (α) value at the rate minimum between the two peaks of each of these curves is shown in Table I.

For samples of a particular size, the rate minimum between the two peaks shifts to an earlier position as a higher reaction temperature is used. Table II illustrates the α 's at the rate minima as a function of the reaction temperature for 270-325 mesh samples.

TABLE I

Reaction temperature 604°K

<u>particle size</u> <u>(mesh)</u>	<u>α at min</u>
45-60	0.034
100-115	0.057
115-150	0.088
150-170	0.13
170-200	0.14
200-270	0.15
270-325	0.21
very fine powder	1.00

TABLE II

Sample particle size 270-325 mesh

<u>react temp. (°K)</u>	<u>α at min</u>
600	0.27
602	0.25
604	0.21
606	0.19
608	0.16
610	0.12
612	0.074
614	--

With the above observations one might suspect that Na_2HPO_4 may react with aluminum. Since the smaller the particle size the greater the contacting surface between the sample and the aluminum pan, if the first hump is from the reaction of the sample and aluminum, of course the first hump will become larger as a smaller particle size is used. However the same results were obtained by pressing down a finely powdered silica layer to separate the direct contact between the sample and the aluminum pan. So we know that the reaction shift to an earlier time is independent of the container.

B. Separation of the Reaction Stages

If we let the sample of 40-65 mesh react at a low temperature (say 580°K), a curve resembling the first hump in Fig. 7a is obtained. The initial reaction rate is fast and reaches the maximum in the first minute. The reaction rate drops down gradually and becomes almost equal to zero after reacting for six minutes. However the reaction has not stopped at this point, it will keep going for hours to complete the decomposition. No second hump like Fig. 7a appears. If we change the reaction temperature to 604°K after the sample has reacted at 580°K for six minutes or more, a curve resembling the second hump in Fig. 7a is obtained (Figure 8). Samples of other particle sizes show similar results. For smaller particle sizes a longer time is required to eliminate the first hump, and the area under the first hump is greater. This result indicates that reaction of Na_2HPO_4 at higher

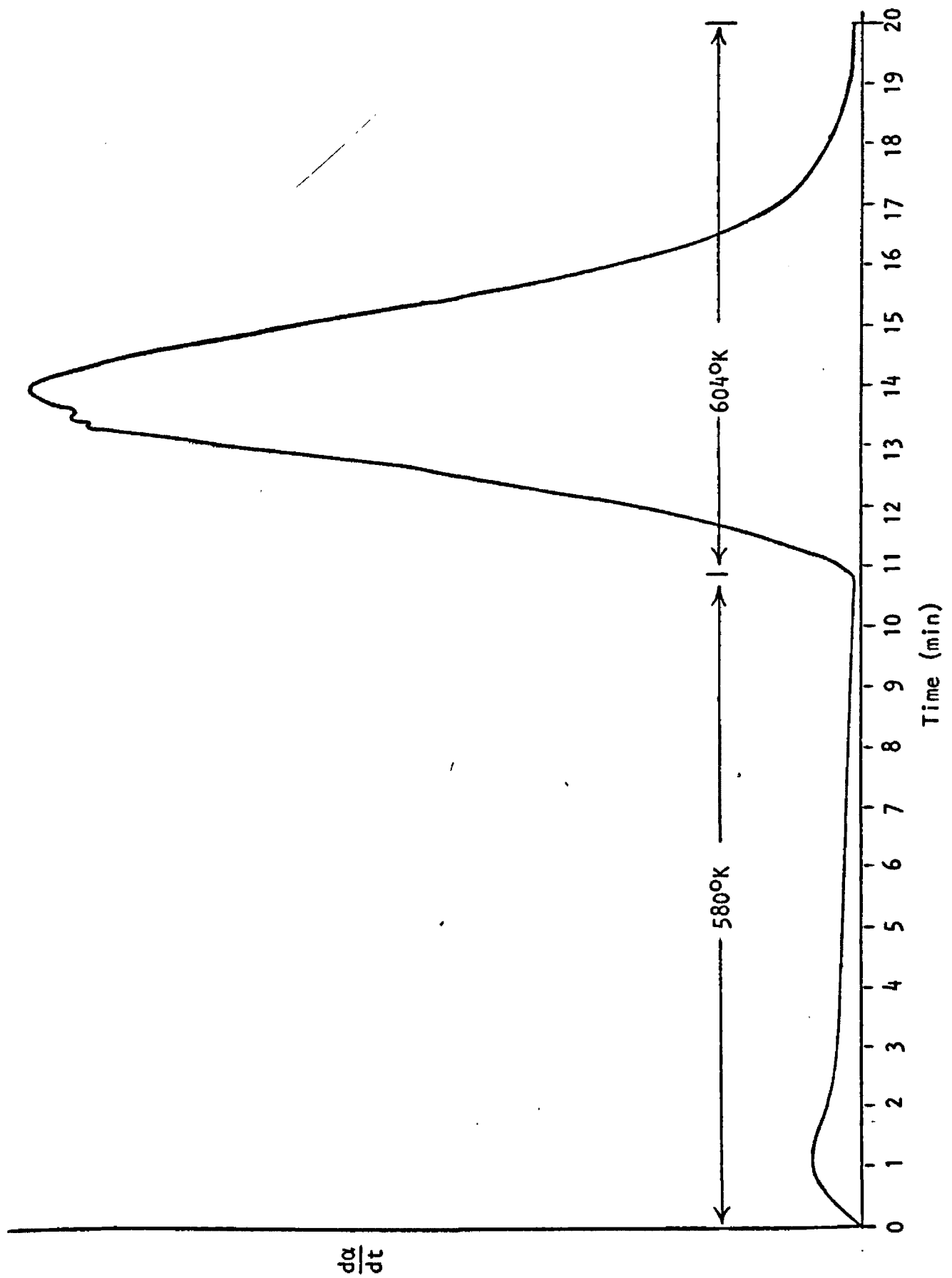


Figure 8-- Na_2HPO_4 held at 580°K for 11 min. then temp. increased to 604°K.

temperatures (596°K or higher) involves a combination of two processes, one that can occur at a lower temperature, another requiring higher temperatures.

C. Kinetic Studies for Samples of 40-65 mesh

If we allow the samples of 40-65 mesh to react at 580°K for 10 to 15 minutes, and then change to a higher temperature (406-620°K), the minor reaction step is separated from the main reaction (cf. previous section). All runs in this section were carried out this way. The data obtained at the higher reaction temperature are characteristic of an autocatalytic reaction followed by a decay process, producing a maximum in the reaction rate. Autocatalytic expressions, such as the Erofeev Equation, Power Law and Prout-Tompkins Equation, were tested against our data. Table III shows the data obtained at 608°K. Table III also presents values of various functions used to test the different kinetic equations described below.

1. Power Law. As shown in equation 11 obtained earlier, the expression of the Power Law is

$$\alpha = Ct^n$$

To test this expression we plot $\log \alpha$ against $\log t$ (Fig. 9A). This expression fits only the very beginning of the reaction ($\alpha < .30$). Note that because this plot is vs. $\log t$, the α scale on Fig. 9 does not apply to curve A.

2. Prout-Tompkins Equation. We test for Prout-Tompkins kinetics (equation 24, obtained earlier)

TABLE III
 Reaction of Na_2HPO_4 (40-65 mesh) at 608°K

<u>Time (min.)</u>	<u>α</u>	<u>$\log t$</u>	<u>$\log \alpha$</u>	<u>$\log\left(\frac{\alpha}{1-\alpha}\right)$</u>	<u>$[\log\left(\frac{1}{1-\alpha}\right)]^{\frac{1}{2}}$</u>
0.400	.0049	-.398	-2.310	-2.310	.0458
0.600	.0166	-.222	-1.780	-1.775	.0849
0.800	.0451	-.0969	-1.346	-1.326	.141
1.00	.0979	.000	-1.009	-.965	.211
1.20	.181	.0792	-.742	-.655	.294
1.40	.281	.146	-.551	-.408	.379
1.60	.390	.204	-.409	-.194	.463
1.80	.501	.255	-.301	.0008	.549
2.00	.605	.301	-.219	.184	.635
2.20	.699	.342	-.155	.367	.723
2.40	.780	.380	-.108	.549	.811
2.60	.846	.415	-.0728	.738	.901
2.80	.894	.447	-.0487	.925	.987
3.00	.930	.477	-.0316	1.12	1.07
3.20	.952	.505	-.0214	1.30	1.15
3.40	.968	.532	-.0142	1.48	1.22
3.60	.978	.556	-.0098	1.64	1.30
3.80	.985	.580	-.0068	1.80	1.35

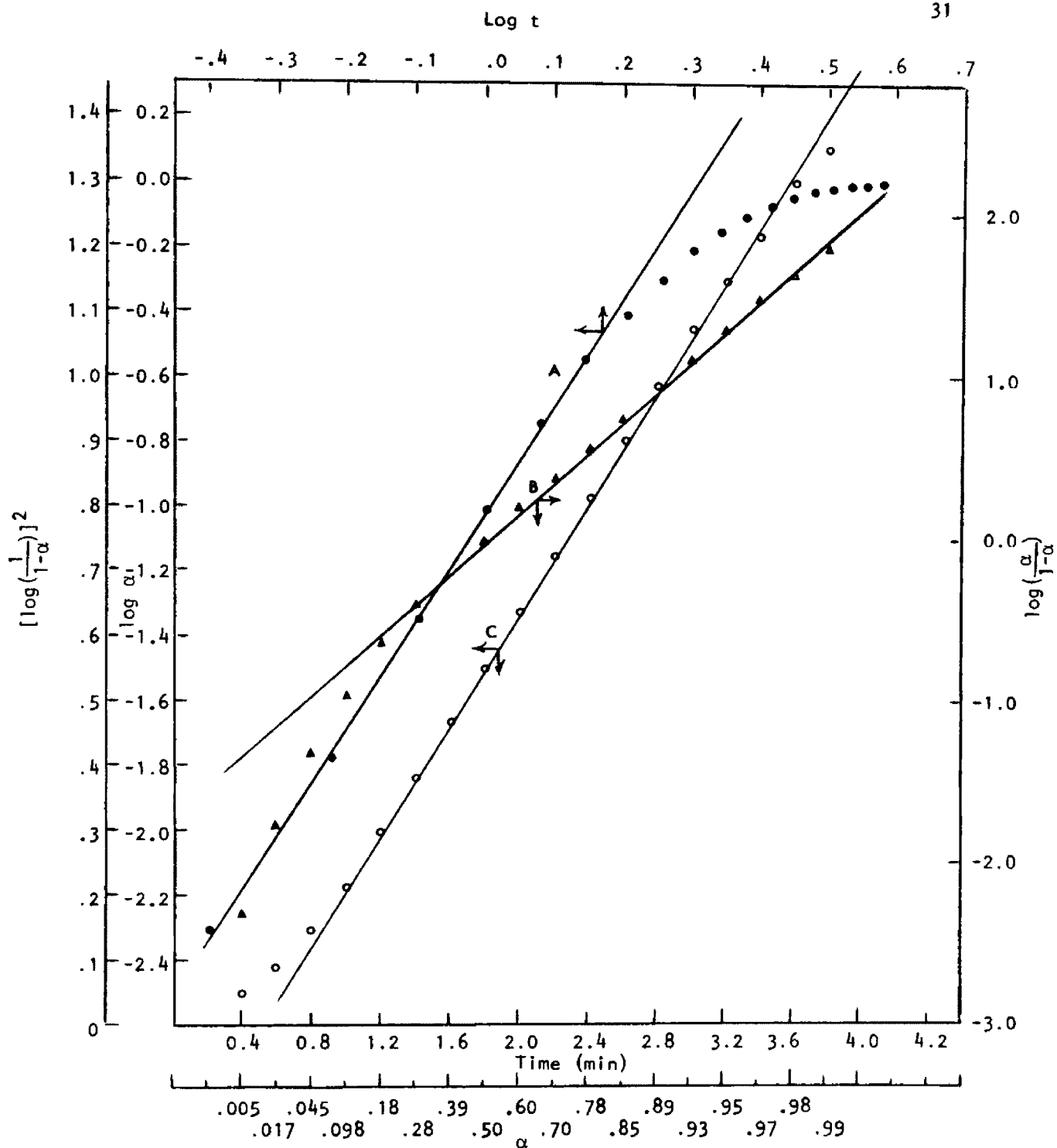


Figure 9--KINETIC EXPRESSION OF Na_2HPO_4 (40-60 mesh) at 608°K

- A ● Power Law $\log \alpha$ vs. $\log t$
- B ▲ Prout-Tompkins Equation $\log(\frac{\alpha}{1-\alpha})$ vs. t
- C ○ Erofeev Equation $[\log(\frac{1}{1-\alpha})]^2$ vs. t

$$\log\left(\frac{\alpha}{1-\alpha}\right) = kt + \text{constant}$$

by plotting $\log\left(\frac{\alpha}{1-\alpha}\right)$ against time (Fig. 9B). This formula does not fit the acceleratory period (before the max. of the $\frac{d\alpha}{dt}$ curve) of this reaction. However it does fit the decay period, and Prout-Tompkins k values for the decay period at various temperatures were calculated. Table IV shows these k values and the α range in which this expression holds. These k values do not give an acceptable Arrhenius plot.

TABLE IV

Prout-Tompkins expression for Na_2HPO_4 (40-65 mesh)

<u>react. temp.</u> <u>(°K)</u>	<u>k (min⁻¹)</u>	<u>α range</u>
606.0	1.65	.33-.99
608.0	2.15	.28-.98
610.0	2.69	.38-.96
612.0	2.98	.30-.93
614.0	3.75	.35-.94
616.0	4.55	.34-.89
618.0	5.71	.32-.81

3. Erofeev Equation. The best fit for our data was found to be the Erofeev Equation (eq. 14) with n equal to 2

$$\log\left(\frac{1}{1-\alpha}\right) = (kt)^2 \quad (30)$$

A straight line is obtained by plotting $[\log\left(\frac{1}{1-\alpha}\right)]^{\frac{1}{2}}$ against time (Fig. 9C). This equation fits almost the entire decomposition curve at every temperature studied. The rate constant, k, can be calculated from the slope of this straight line. In Table V are

given the rate constants at different temperatures together with the range of α in which the Erofeev Equation holds. The Arrhenius plot is shown in Figure 10, and the activation energy, ΔE^* , is found to be 74 ± 5 kcal/mole.

TABLE V
Erofeev expression for Na_2HPO_4 (40-65 mesh)

<u>react. temp</u> (°K)	<u>k</u> (min ⁻¹)	<u>α range</u>	<u>log k</u>	<u>$\frac{1}{T} \times 10^3$</u>
606.0	.493	.045-.98	-.307	1.650
608.0	.653	.098-.95	-.186	1.645
610.0	.787	.078-.93	-.104	1.639
612.0	.930	.059-.93	-.0318	1.634
614.0	1.17	.093-.92	.0679	1.629
616.0	1.43	.12-.89	.155	1.623
618.0	1.67	.079-.87	.222	1.618

It is observed from Table V that the equation holds in a range $.1 < \alpha < .9$. Fit throughout the entire run cannot be expected. Since about half a minute is required for the sample to reach the desired reaction temperature, we do not expect the equation to fit the very early time of the reaction. In the later time of the decomposition, nucleus forming sites have been depleted, so the equation does not apply. Accumulated error in the integration of $\frac{d\alpha}{dt}$ vs. t to obtain α values also prevents one from expecting a good fit at high α values.

As the sample particle size used is decreased the fraction of reaction represented by the second hump becomes smaller, and

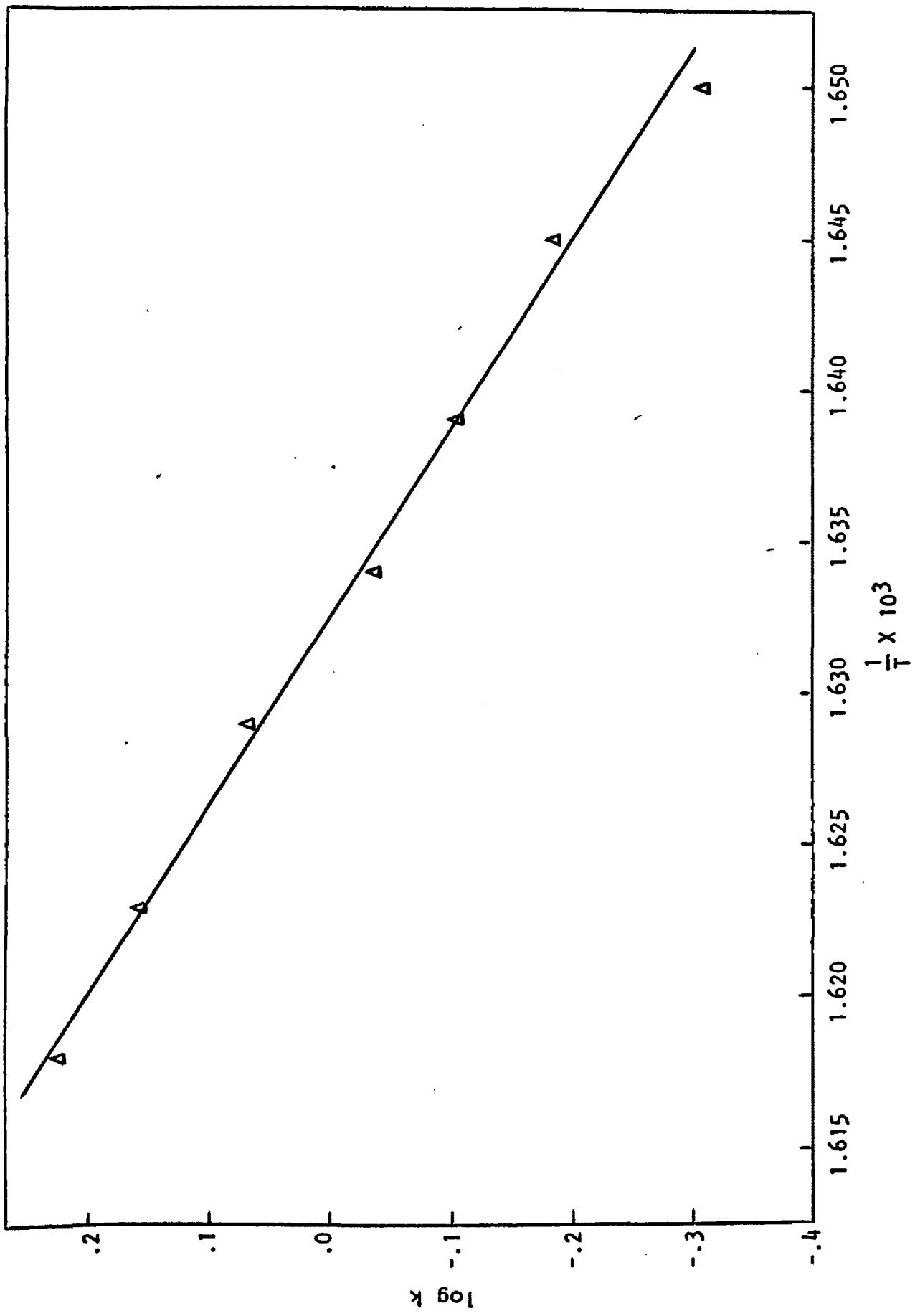


Figure 10--Arrhenius plot for Na₂HPO₄ (40-65 mesh)

the experimental conditions for resolving the two humps become more critical. It has not been possible to get useful data for the second reaction with smaller particle sizes than 40-65 mesh.

D. Kinetic Studies for Samples of Very Fine Powder

We have seen that the area under the first hump of a thermogram increases as sample particle size decreases; finally a one-hump curve is obtained for very fine powder. It is reasonable that the nature of the first hump in other thermograms can be understood by studying this one-hump curve.

As shown in Figure 11, the reaction of a sample of very fine powder has no induction period. The initial reaction is extremely fast and reaches a maximum rate within half a minute. This is essentially the time required for the sample to reach the reaction temperature. The decay period constitutes virtually the entire curve. Kinetic expressions standardly employed for reactions with a very fast initial rate, such as diffusion control and spherical interfacial expressions, were tried to fit our data. Table VI illustrates data obtained at 588°K and values of different functions used to test the kinetic equations. Statements concerning each test are given below.

1. Spherical Interfacial. From equation 26, obtained earlier, the spherical interfacial expression is

$$(1-\alpha)^{\frac{1}{3}} = 1 - \frac{k}{R} t$$

We tested this expression by plotting $(1-\alpha)^{\frac{1}{3}}$ against time. This

TABLE VI

Reaction of Na_2HPO_4 (very fine powder) at 588°K

<u>Time (min)</u>	<u>α</u>	<u>$(1-\alpha)^{\frac{1}{3}}$</u>	<u>$[1-(1-\alpha)^{\frac{1}{3}}]^2$</u>	<u>$\log\left(\frac{1}{1-\alpha}\right)$</u>
.280	.0687	.976	.00055	.0311
.680	.240	.913	.00764	.119
1.08	.365	.858	.0198	.197
1.48	.456	.816	.0337	.264
1.88	.528	.778	.0491	.326
2.28	.588	.744	.0641	.385
2.68	.641	.712	.0833	.445
3.08	.688	.678	.103	.506
3.48	.729	.646	.124	.568
3.88	.766	.617	.147	.631
4.28	.799	.586	.172	.697
4.68	.828	.555	.198	.765
5.08	.853	.528	.224	.834
5.48	.876	.499	.251	.907
5.88	.896	.472	.279	.982
6.28	.912	.445	.306	1.06
6.68	.928	.415	.341	1.14
7.08	.941	.390	.373	1.23
7.48	.951	.367	.403	1.31
7.88	.961	.340	.437	1.40
8.28	.968	.316	.468	1.50
8.68	.974	.296	.497	1.59
9.08	.979	.277	.527	1.67
9.48	.984	.254	.562	1.79
9.88	.988	--	.600	1.91

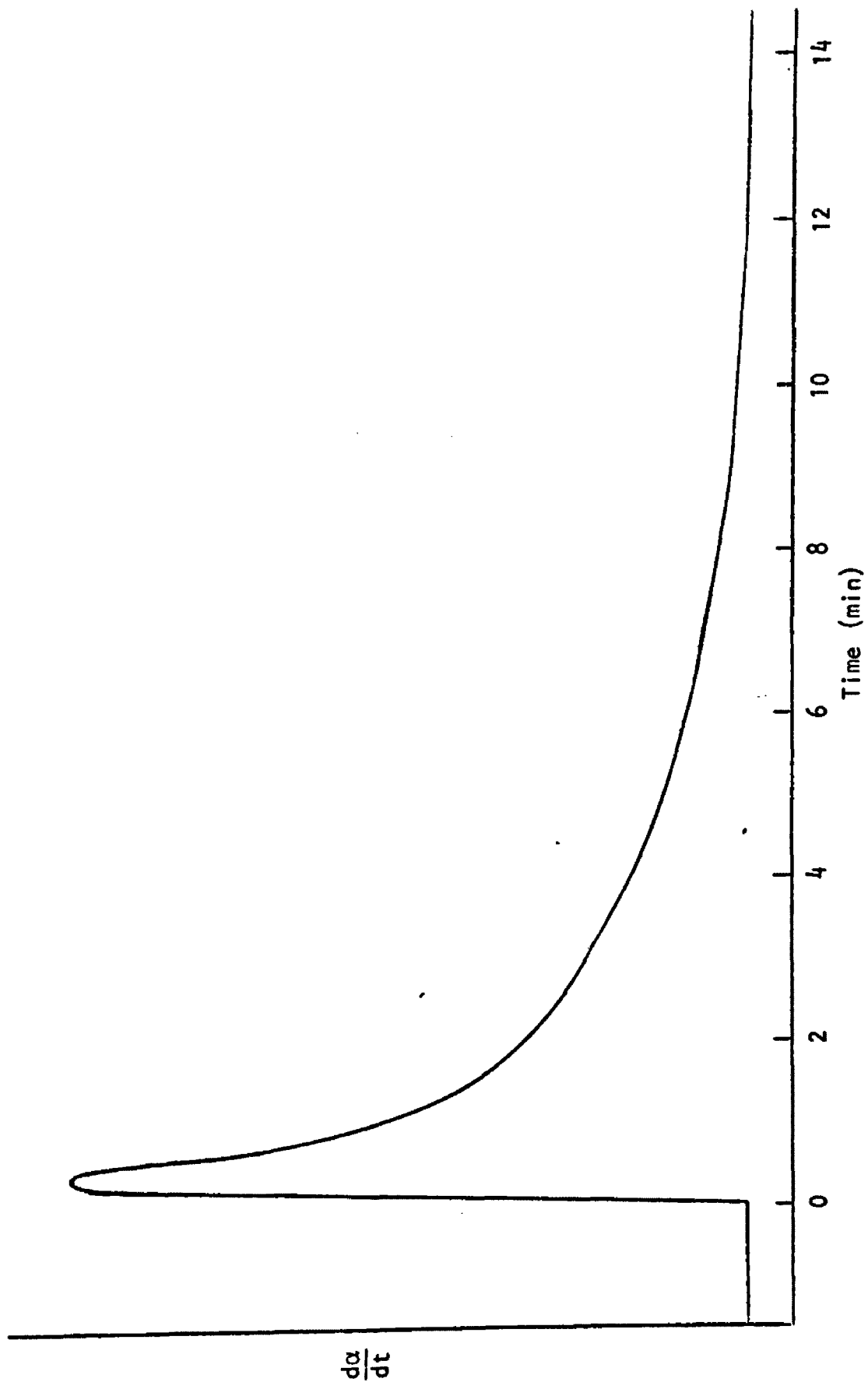


Figure 11--Thermogram of Na_2HPO_4 (very fine powder) at 588°K

expression does not fit our data as shown in Figure 12A.

2. Diffusion control. From equation 27 the diffusion control expression is

$$[1 - (1-\alpha)^{\frac{1}{3}}]^2 = \frac{k}{R^2}t$$

To test this expression we plot $[1 - (1-\alpha)^{\frac{1}{3}}]^2$ against time (Fig. 12B), this formula fits at the very end of the decay period ($\alpha \geq .90$).

3. The best fit to this decay curve is found for the equation

$$\log\left(\frac{1}{1-\alpha}\right) = kt \quad (31)$$

The rate constant k can be obtained from the slope of a plot of $\log\left(\frac{1}{1-\alpha}\right)$ against time (Fig. 12C). Values of k at various temperatures are entered in Table VII. An Arrhenius plot is shown in Figure 13, and the activation energy is found to be 42 ± 4 kcal/mole.

TABLE VII
Decay process of Na_2HPO_4 (very fine powder)

<u>react. temp. ($^{\circ}\text{K}$)</u>	<u>k (min^{-1})</u>	<u>α range</u>	<u>$\log(k \times 10^2)$</u>	<u>$\frac{1}{T} \times 10^3$</u>
572.0	.124	.38-.95	1.093	1.748
576.0	.173	.34-.94	1.238	1.736
580.0	.242	.34-.90	1.384	1.724
584.0	.292	.30-.87	1.465	1.712
588.0	.375	.24-.87	1.574	1.701
592.0	.461	.27-.85	1.664	1.689
596.0	.606	.19-.83	1.783	1.678
598.0	.677	.20-.87	1.831	1.672
600.0	.682	.17-.88	1.834	1.667

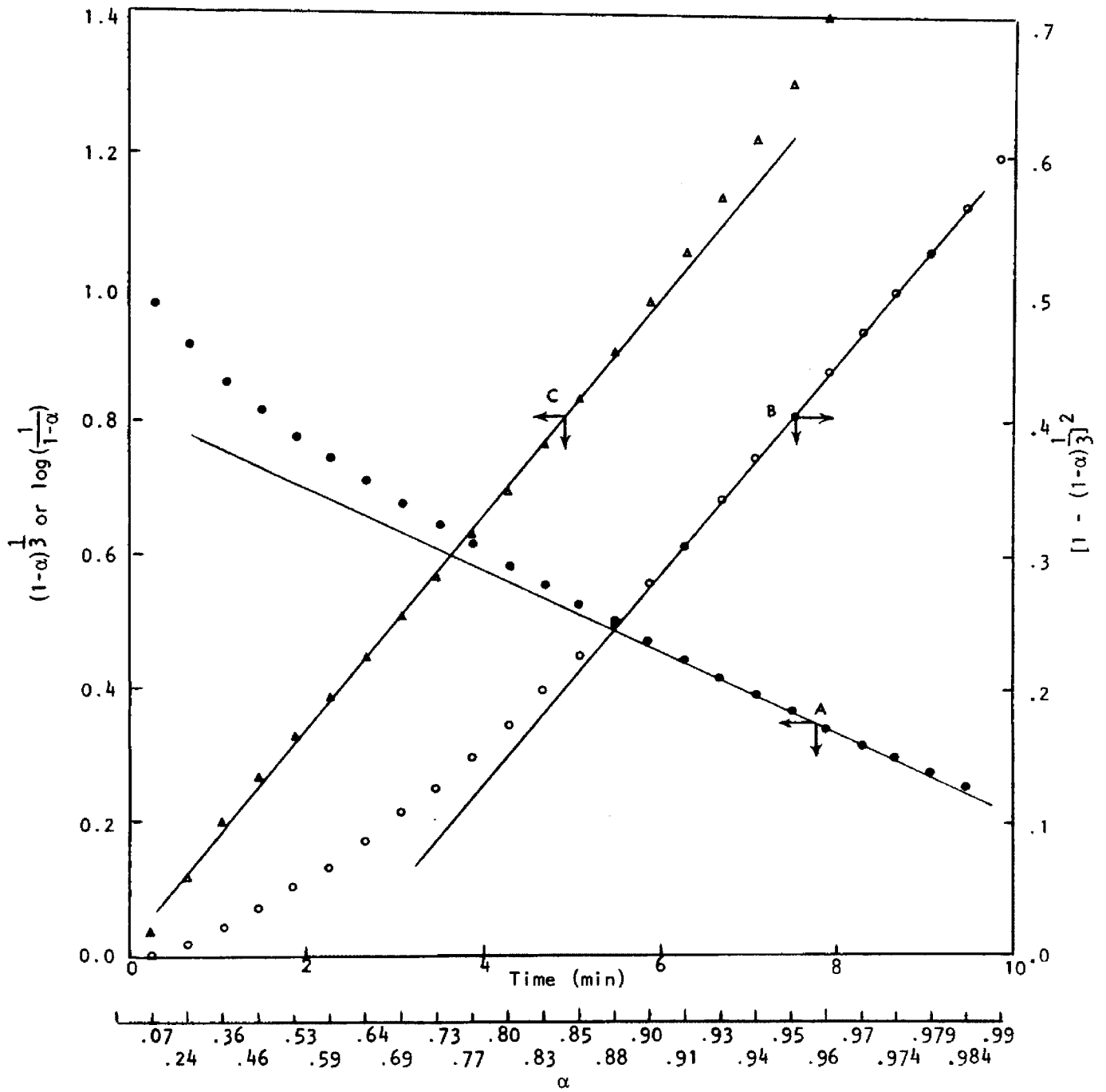


Figure 12--Kinetic Plot of Na_2HPO_4 (very fine powder) at 588°K

- A ● Spherical interfacial $(1-\alpha)^{\frac{1}{3}}$ vs. t
 B ○ Diffusion control $[1 - (1-\alpha)^{\frac{1}{3}}]^2$ vs. t
 C ▲ Decay process $\log(\frac{1}{1-\alpha})$ vs. t

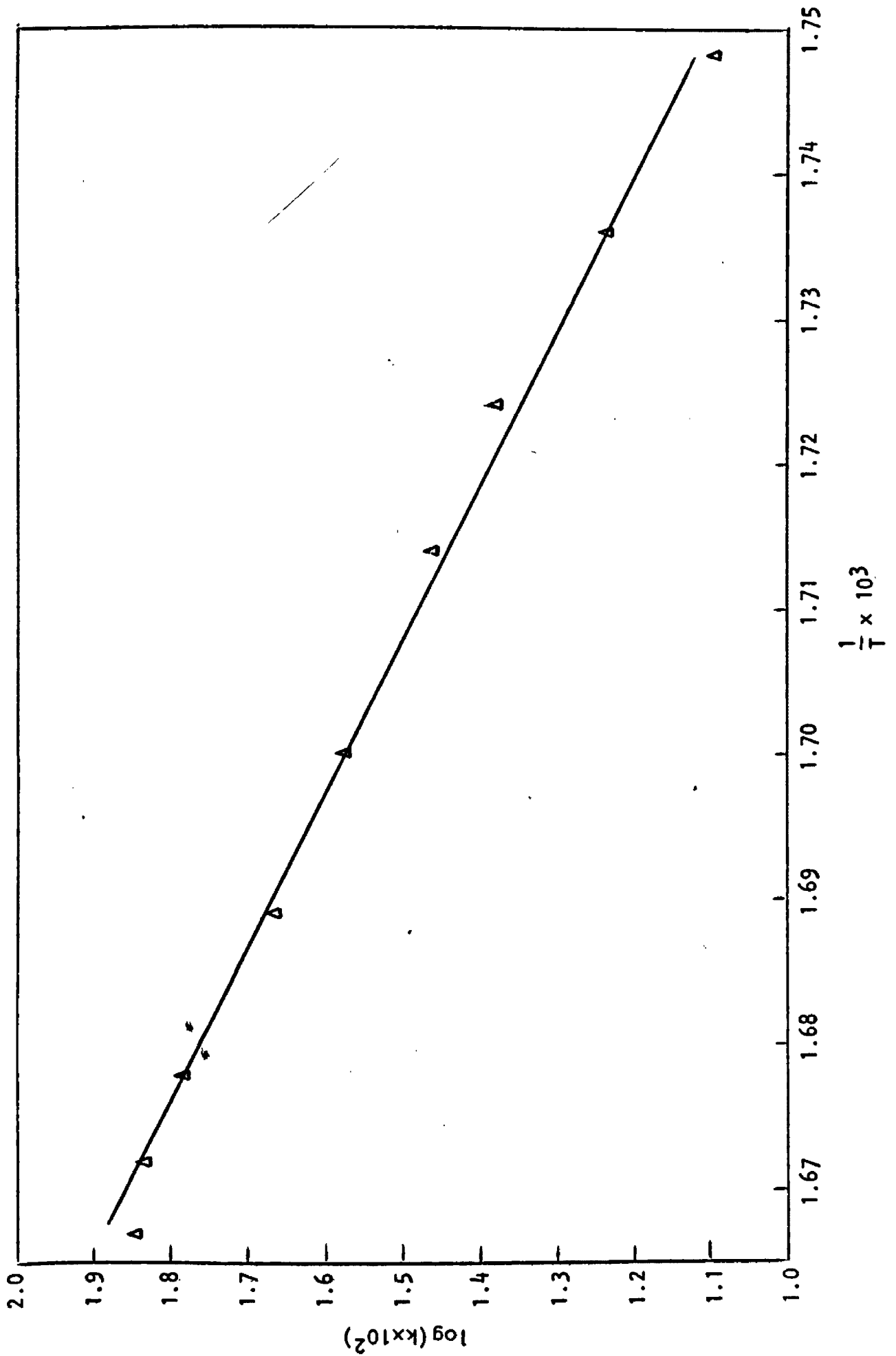


Figure 13--Arrhenius plot for Na_2HPO_4 (very fine powder)

Equation 31 does not hold for small α values, this can be seen from the differential form of the equation

$$\frac{d\alpha}{dt} = ke^{-kt} \quad (32)$$

According to equation 32 the absolute maximum is at time zero; this is quite different from the actual case. Therefore equation 31 can only apply to the decay period of the reaction. Due to experimental limitations: (a) the impossibility of bringing the sample to the reaction temperature instantaneously and (b) delays in the response of the rate measuring equipment, the experimental curve required a finite period of time to show true decay kinetics. No decay kinetic expression can fit the data until the curve has passed not only its maximum, but also has passed the inflection following the maximum. Although both of these points occur early in time, because of the high initial rate these points are relatively late in α . For example, in the run illustrated in Figure 11, the maximum and the inflection following the maximum occur at 0.36 and 0.48 minutes, respectively, out of a run lasting about thirteen minutes, but occur at α values of .11 and .16, respectively. Equation 31 fits the data as early in the run as can be expected, and much earlier than do alternate expressions.

Due to accumulated error in the integration of the $\frac{d\alpha}{dt}$ vs. t data to obtain α values, no expression should be expected to fit the very late period of the reaction.

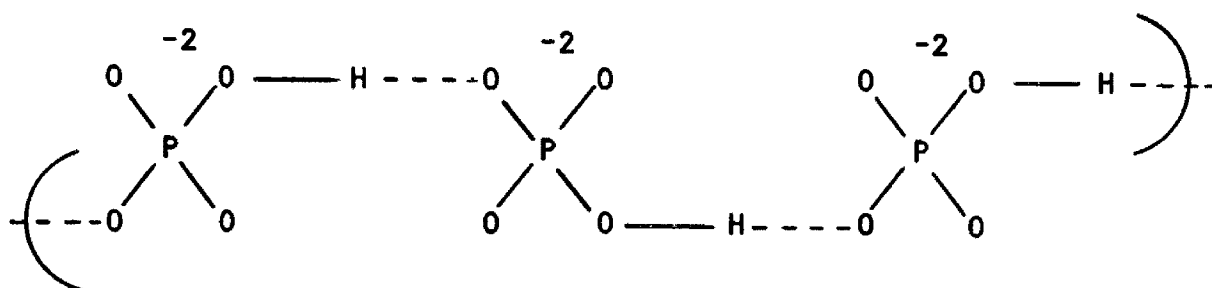
VI. DISCUSSION

A. The Erofeev Mechanism

The exponent n in the Erofeev expression is the sum of the number of steps (β) required to produce a growth nucleus and the number of dimensions (λ) in which the reaction propagates from that nucleus. In the decomposition of Na_2HPO_4 by the Erofeev mechanism n has the value 2. Since grinding increases the initial rate by an effect other than particle size reduction, the effect of grinding must be due to an increase in the nucleation rate. The Erofeev mechanism, then, in samples that have been ground little, must involve a nucleation process of at least one step. The change, following the rate maximum, to a well-defined decay period requires a propagation process in at least one direction. It follows that the reaction must involve a one-step nucleation and one-dimensional propagation. It is not required that the propagation be linear; the propagation chain might be a random walk, for example. However, the one-dimensional propagation rules out chain branching, and this makes a random walk unlikely. If the chains are then considered to propagate in straight line, these lines cannot all be parallel, as the decay period arises from an overlap term attributed to chain termination arising from encounters between chains.

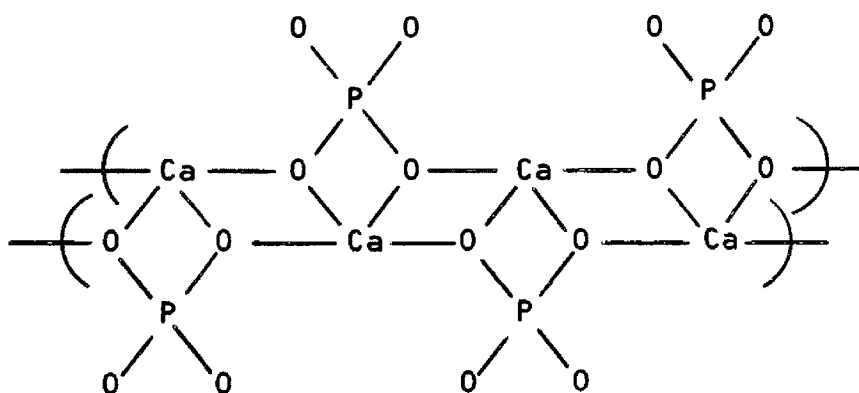
The crystal structure of Na_2HPO_4 has not been determined. It is interesting, however, that hydrogen phosphates are known to have hydrogen bonds between the anions. In any monohydrogen

phosphate the single hydrogen atom per phosphate ion is just enough to establish hydrogen-bonded anion chains.



Such a hydrogen-bonded chain has been proposed in one crystal structure study of CaHPO_4 .¹⁰

For only two anhydrous monohydrogen phosphates have the crystal structures been determined. In both of these a chain-type cation-anion coordination has been reported. For CaHPO_4 , a ribbon-like double chain structure has been reported.¹¹



For BaHPO_4 , a simple single chain structure has been reported.³



The reaction chains in the Erofeev mechanism might be either along hydrogen-bonded chains or cation-anion chains.

B. The Logarithmic Decay Mechanism

We have seen the decomposition of Na_2HPO_4 involves a wholly decay type process in addition to the Erofeev mechanism. Apparently these two processes are not independent: (1) the first peak (the wholly decay process) becomes larger at the expense of the second as a sample of smaller particle size is used, and (2) for any particle size, the entire reaction can be carried out as part of the first reaction. A question arises concerning the relationship between the Erofeev mechanism for large particles and the decay process for smaller particles. For answers to this and an understanding of the mechanism that leads to the kinetics for the very fine powder, let us examine the results obtained from the samples of very fine particle.

1. Suppose that the particles of very fine powder are so small that a particle is completely converted to product soon after nuclei are formed in that particular particle. That is, propagation is not a factor in the kinetics for the reaction, and the reaction rate is then determined by nucleation kinetics. This rate is dependent upon the amount of reactant left at time t , assuming potential nucleus sites are uniformly distributed throughout the sample.

$$\frac{d\alpha}{dt} = k(1-\alpha)$$

so that

$$\log\left(\frac{1}{1-\alpha}\right) = kt \quad (33)$$

which is the kinetic expression we have found applies to samples of very fine powder.

With this decay process for very fine particles and the Erofeev mechanism for big particles, the dependence on particle size of the kinetics for the decomposition process can be explained as follows. Grinding the sample into smaller particles produces scratches on the surface of the crystals. Assuming reaction at a scratch is easiest, reaction next to $P_2O_7^{-4}$ (i.e., propagation) is next easiest, and ordinary potential nuclei sites are hardest to react:

(a) 40-65 mesh sample--very few scratches. Kinetics depend on the slow, hard ordinary nucleation step and subsequent propagation. However, there are a few scratches that lead to a minor first step. Because the particles are large, however, the propagation chain is long enough that the first step does not have the simple kinetics of the very fine powder. And, possibly there is some interference of chains.

Nucleation kinetics for reaction starting at a scratch

are $\frac{dN_s}{dt} = k_s(N_{O_s} - N_s)$. Nucleation kinetics for

reaction starting at ordinary potential nuclei are

$\frac{dN}{dt} = kN_0$ where N_s is number of nuclei from scratches

at time t ; N_{O_s} is the number of potential nuclei at scratches and N_O the number of ordinary potential nuclei sites. k_s , The rate constant for nucleation at scratches, is assumed to be much larger than k_o , the rate constant for nucleation at ordinary potential nuclei.

(b) As the particle size is reduced, more of reaction is derived from nuclei formed at scratches as the result of an increase in the value N_{O_s} , and interference between chains becomes less important in the kinetics, because the chains are short anyway. For intermediate particle size ranges, the observed dependence of $\frac{d\alpha}{dt}$ on t consists of two overlapping steps. The first step has the decay kinetics of very fine powder, and there follows a second step of Erofeev mechanism as the sites near scratches (N_{O_s}) are used up. Figure 14 shows how these two steps can combine to give the observed kinetics.

(c) For very fine particles, the kinetics are simply the nucleation kinetics for the first step.

2. From another viewpoint, suppose that surface defects, such as scratches, serve as particularly effective nuclei for decomposition, so that reaction propagates from scratches instantaneously, with no kinetics of nucleation to be considered. The rate of decomposition is then governed by the one-dimensional growth of

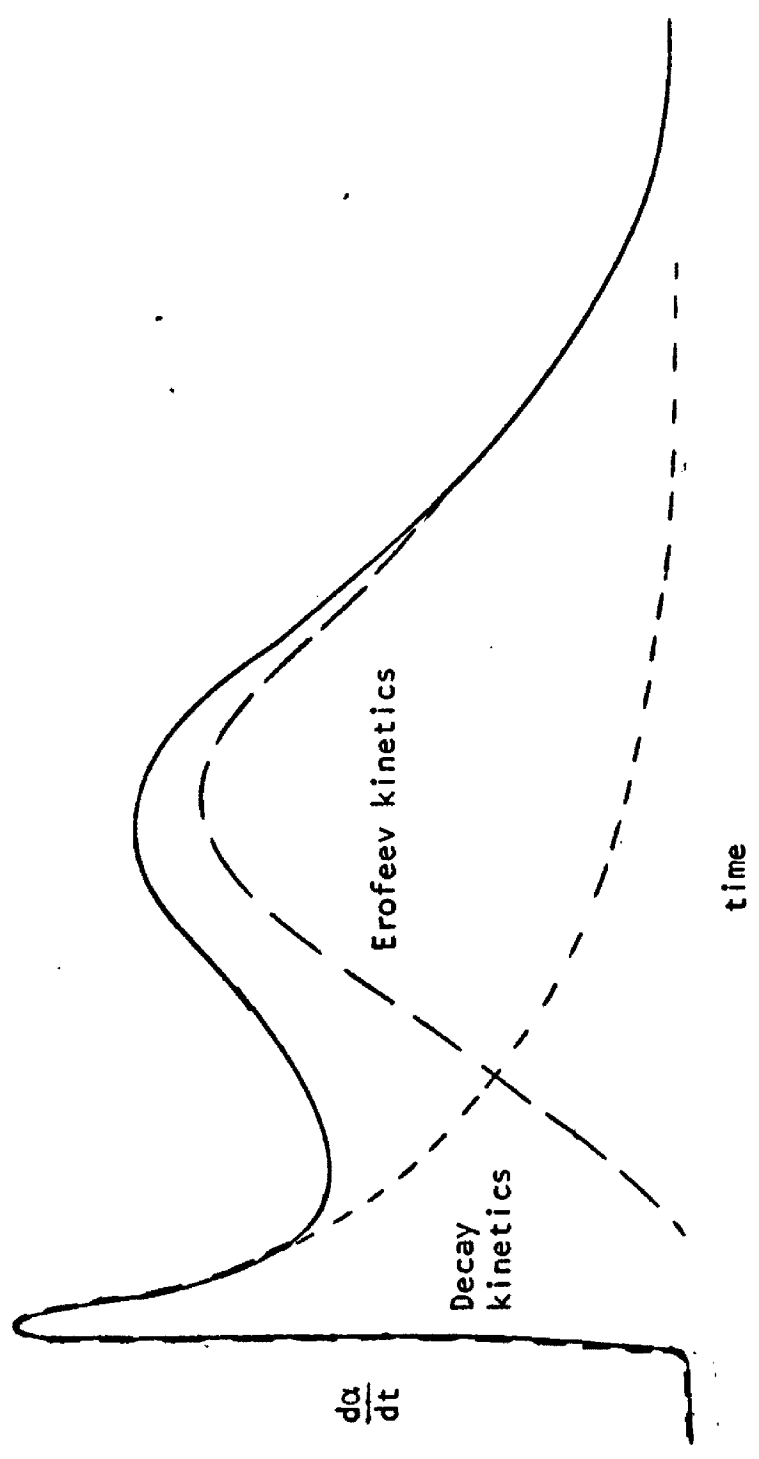


Figure 14--Thermogram obtained from a combination of the decay and Erofeev kinetics.

these nuclei and the interference of these propagation chains with each other. In this case the kinetic equation will be

$$\alpha = k_g N_0 t$$

and

$$\frac{d\alpha}{dt} = k_g N_0 \quad (34)$$

Allowing for overlap in the usual way we have

$$\frac{d\alpha}{dt} = k_g N_0 (1-\alpha) \quad (35)$$

which on integration gives

$$\log\left(\frac{1}{1-\alpha}\right) = k_g N_0 t \quad (36)$$

This is the same equation that we have found applies to samples of very fine powder. The hardest part of the decomposition is forming a growth nucleus. Once the nuclei are formed by grinding of a crystal, these nuclei will start to react at a temperature prior to the nucleation in the remainder of the crystal. Thus

(a) 40-65 mesh sample--the reaction follows mainly the Erofeev mechanism. The minor first step is due to the propagation of some previously formed nuclei in scratches. Because the particle is big and very few scratches are on the surface of the crystal, overlap in the propagation of these activated nuclei is less possible; unlike the decomposition curve of very fine powder the first hump is small and flat.

(b) As particle size is reduced, more activated nuclei are formed on the surface of the crystals. Overlap in the propagation of these nuclei is possible; the first step follows the propagation kinetics of very fine powder. The unscratched portion still follows the Erofeev mechanism (Fig. 14).

(c) For very fine particles, the kinetics are simply those of one-dimensional propagation, with termination from overlap of the chains.

From both viewpoints, the increasing importance of the first, wholly decay step as one studies progressively smaller particles is attributed to an increasingly scratched particle surface. Both viewpoints relate this first step to the Erofeev kinetics of the main step. The first viewpoint attributes the decay kinetics to (a) the introduction of a relatively fast nucleation process for the kinetics of which the consumption of potential nuclei cannot be ignored and to (b) the elimination of propagation as a kinetic factor due to the small size of the particles. The second viewpoint attributes the decay kinetics to (a) the introduction of scratches that serve as nuclei, eliminating nucleation as a kinetic factor leaving (b) the propagation kinetics as the resultant observed kinetics.

C. Interpretation of Activation Energies

In the study of samples of 40-65 mesh the rate constants obtained by plotting $[\log(\frac{1}{1-\alpha})]^{\frac{1}{2}}$ against time are in fact equal to $(\frac{N_0 k_1 k_g}{2})^{\frac{1}{2}}$, where k_1 and k_g are rate constants for nucleation

and propagation respectively. Consequently the activation energy (74 kcal/mole) obtained for this reaction is a combination of ΔE_1^* of nucleation and ΔE_g^* of propagation. The exact relationship can be derived from Arrhenius equations for nucleation and propagation. Let

$$k_1 = A_1 e^{-\Delta E_1^*/RT} \quad (37)$$

and

$$k_g = A_g e^{-\Delta E_g^*/RT} \quad (38)$$

where A_1 and A_g are frequency factors for nucleation and propagation respectively. R is the gas constant and T temperature. Combining the above equations we obtain

$$(k_1 k_g)^{\frac{1}{2}} = (A_1 A_g)^{\frac{1}{2}} e^{-\frac{\Delta E_1^* + \Delta E_g^*}{2RT}} \quad (39)$$

Since the observed rate constant, k , is equal to $(\frac{N_0}{2} k_1 k_g)^{\frac{1}{2}}$ and the factor $(\frac{N_0}{2})^{\frac{1}{2}}$ does not affect the slope obtained by plotting $\log k$ vs. $\frac{1}{T}$, we see from equation 39 that

$$\Delta E_{\text{observed}}^* = \frac{\Delta E_1^* + \Delta E_g^*}{2} = 74 \text{ kcal/mole} \quad (40)$$

thus

$$\Delta E_1^* + \Delta E_g^* = 148 \text{ kcal/mole} \quad (41)$$

For the decay kinetics observed for very fine powder we have found an activation energy of 42 kcal/mole. In the preceding

section we presented two mechanisms consistent with the decay kinetics. From the viewpoint of the first of these mechanisms, attributing the kinetics to new nucleation kinetics, 42 kcal/mole is the activation energy for this new nucleation process occurring at scratches. On the basis of the second mechanism, attributing the kinetics to one-dimensional chain propagation and overlap, 42 kcal/mole is the activation energy for the propagation step in the Na_2HPO_4 decomposition. Depending on the mechanism for the very fine powder decomposition, then, two activation energy assignments are possible. These are given in Table VIII.

TABLE VIII
Activation Energies in the Na_2HPO_4 Decomposition

Process	1* Viewpoint	2*
Nucleation at scratches	42 kcal/mole	very small
Nucleation at ordinary potential sites	} Total 148 kcal/mole	106 kcal/mole
Chain propagation		42 kcal/mole

*These viewpoints are explained in Section B of the associated text.

In essence, the two viewpoints on the very fine powder decomposition mechanism differ in the activation energy assigned to the decomposition at a scratch. If this process is assigned an activation energy appreciably greater than zero, then the kinetics of nucleation

at scratches must be considered; if this activation energy is essentially zero, then this process is not involved in the kinetic expression, and the observed kinetics are propagation kinetics.

No choice between these viewpoints can be made without further study. Highly desirable would be a visual study of the kinetics of propagation in single crystals that had been artificially nucleated on a single face by scratching and impregnating the face with $\text{Na}_4\text{P}_2\text{O}_7$. If artificial nucleation could be induced in this way, the propagation activation energy could be determined unambiguously.⁷

SUMMARY

The decomposition of Na_2HPO_4 has been studied at 300-345°C



By means of a thermal conductivity cell in the stream of carrier gas leaving the reaction zone the rate of the evolution of the constitutional water was measured during isothermal runs. It was found that samples of large particle size (40-65 mesh) follow the Erofeev kinetic equation with $n = 2$

$$\log\left(\frac{1}{1-\alpha}\right) = (kt)^2$$

This exponent indicates a mechanism of a single nucleation step, followed by one-dimensional chain-type propagation. A procedural activation energy of 74 ± 5 kcal/mole was found. Interpretations of this value were offered.

Samples of very fine powder follow the decay kinetic expression

$$\log\left(\frac{1}{1-\alpha}\right) = kt .$$

An activation energy of 42 ± 4 kcal/mole was found for this step. Two possible mechanisms were proposed to explain the decay kinetics.

For intermediate size particles, a combination of the above two kinetic expressions is followed.

BIBLIOGRAPHY

1. Avrami, M., J. Chem. Phys. 7, 1103 (1939); 8, 212 (1940); 9, 177 (1941).
2. Bagdasar'yan, Kh. S., Acta phys-Chem. U.R.S.S. 20, 441 (1945).
3. Burley, G., J. Res. Nat'l Bur. Stds. 60, 23 (1958).
4. Erofeev, B. V., Compt. rend. acad. sci. U.R.S.S. 52, 511 (1946).
5. Garner, W. E., Chemistry of the Solid State, Chapter 7, Butterworths Scientific Publications, London (1955).
6. Garner, W. E. and Hailes, H. R., Proc. Roy. Soc. 139A, 576 (1933).
7. Hume, J. and Colvin, J., Proc. Roy. Soc. 125A, 635 (1929).
8. Instruction Manual--Differential Scanning Calorimeter--1B, Perkin-Elmer Corp., Norwalk, Conn. (1966).
9. Jander, W., Z. anorg. allgem. Chem. 163, 1 (1927).
10. Jones, D. W. and Cruickshank, D. W. J., Z. Krist. 116, 101 (1961).
11. McLennan, G. and Beevers, C. A., Acta Cryst. 9, 579 (1955).
12. Prout, E. G. and Tompkins, F. C., Trans. Faraday Soc. 40, 488 (1944).
13. Topley, B. and Hume, J., Proc. Roy. Soc. 120A, 211 (1928).
14. Watson, E. S., O'Neill, M. J., Justin, J. and Brenner, N., Anal. Chem. 36 (7), 1233 (1964).
15. Young, D. A., Decomposition of Solids, pp. 1-54, Pergamon Press, New York (1966).